Anusandhanvallari
Vol 2020, No.1
December 2020
ISSN 2229-3388

Nano-Dispersed Boron Carbide Reinforced Aluminium Metal Matrix Nanocomposites: Fabrication via Ultrasonic Cavitation-Assisted Casting and Investigation of Microstructural, Mechanical, and Wear Properties

M. Venkatesan[1], D. V. Patel[2]*, Dr. Prashant S. Kadu[3]

[1,2]Department of Mechanical Engineering Sri Satya Sai University of Technology & Medical Sciences, Sehore, Madhya Pradesh, India

[3]Principal, Abha-Gaikwad Patil College of Engineering, Nagpur

Abstract: Aluminium metal matrix nanocomposites (AMNCs) reinforced with nano-scale boron carbide (B4C) particles offer an attractive combination of low density, high specific strength, and superior wear resistance for automotive, aerospace, and structural applications. In this work, nano-B4C particles (average size ~50 nm) were synthesised by high-energy planetary ball milling of commercially available micron-sized B4C powder (0.8 micron) for up to 20 hours under an argon atmosphere. The nano-B4C particles were incorporated into an AA6061 aluminium alloy matrix at volume fractions of 0-2.5 vol.% using an ultrasonic cavitation-assisted casting route operating at 2 kW and 20 kHz. Microstructural characterisation using X-ray diffraction (XRD), scanning electron microscopy (SEM), transmission electron microscopy (TEM), atomic force microscopy (AFM), and energy dispersive spectroscopy (EDS) confirmed a fine, largely uniform dispersion of B4C particles within the aluminium matrix together with an elevated dislocation density at the particle-matrix interface. Mechanical characterisation (Vickers/Brinell hardness, uniaxial tensile testing, IZOD impact testing) and dry sliding wear testing (pin-on-disc) revealed that hardness and tensile strength increased progressively with B4C content up to approximately 2.0 vol.%, beyond which particle agglomeration and micro-porosity degraded properties. Elongation to fracture decreased monotonically with reinforcement content, while nano-reinforced composites consistently outperformed micron-reinforced counterparts in wear resistance and impact toughness at equivalent nominal reinforcement content. These findings support ultrasonic cavitation-assisted casting as a scalable, cost-effective route for producing nano-B4C/AA6061 composites with tailored mechanical and tribological performance for structural lightweighting applications.

Keywords: Aluminium metal matrix nanocomposite; Boron carbide; Ultrasonic cavitation casting; High-energy ball milling; Mechanical properties; Wear resistance

1. Introduction

Metal matrix composites (MMCs) combine a ductile metallic matrix with a hard, stiff reinforcing phase to achieve property combinations unattainable by either constituent alone. Among available matrix metals, aluminium and its alloys are the most widely exploited owing to their low density, good corrosion resistance, high thermal and electrical conductivity, and ease of processing. Aluminium metal matrix composites (AMCs) reinforced with ceramic particles such as silicon carbide (SiC), alumina (Al2O3), and boron carbide (B4C) are extensively employed in automotive, aerospace, and defence applications, where weight reduction without loss of structural performance is a primary design driver[1-4].

Boron carbide is particularly attractive as a reinforcement because of its exceptionally high hardness (third only to diamond and cubic boron nitride), low density (2.52 g/cm3), high melting point, good chemical stability, and large neutron absorption cross-section, which additionally makes B4C-reinforced composites useful for radiation shielding. Refining the reinforcing B4C phase from the conventional micron scale to the nanometre scale allows the resulting nanocomposites to benefit from Orowan strengthening, grain-boundary (Hall-Petch)

strengthening, and thermal-mismatch-induced dislocation strengthening arising from the large difference in coefficient of thermal expansion between Al and B4C[5]. However, achieving a homogeneous dispersion of nanoparticles within a metallic melt is difficult because nanoparticles agglomerate readily under Van der Waals forces and tend to be rejected at the solidification front[6].

Ultrasonic cavitation-assisted casting has emerged as a promising liquid-state processing route for overcoming this dispersion challenge. High-intensity ultrasonic waves transmitted into the melt through a titanium horn generate transient cavitation bubbles; their violent collapse produces localised shock waves and micro-jets that fragment particle clusters and promote wetting between the ceramic reinforcement and the molten aluminium, yielding a more uniform particle distribution than mechanical stirring alone can achieve[7].

While powder metallurgy remains the most widely reported route for producing nano-reinforced aluminium composites, it is comparatively costly and difficult to scale to large, near-net-shape components. Liquid-state processing routes, particularly stir casting and its ultrasonically assisted variant, are inherently more compatible with existing foundry infrastructure and offer a more direct path to industrial adoption, provided the nanoparticle dispersion challenge can be adequately addressed[8-10]. The present work is therefore motivated not only by the mechanical and tribological performance of the resulting nanocomposite but also by the practical demonstration that a scalable, foundry-compatible liquid-state route can achieve a dispersion quality sufficient to realise the strengthening benefits normally associated with powder-metallurgy-processed nanocomposites.

The present study investigates the fabrication of nano-B4C reinforced AA6061 aluminium metal matrix nanocomposites (MMNCs) by combining high-energy ball milling (for nanoparticle synthesis) with ultrasonic cavitation-assisted casting (for composite fabrication). The specific objectives are to: (i) synthesise nano-scale B4C particles from micron-sized feedstock via controlled ball milling and characterise their evolution in particle size, morphology, and crystal structure with milling time; (ii) fabricate AA6061/B4C nanocomposites over a range of reinforcement fractions (0-2.5 vol.%) using ultrasonic cavitation-assisted casting; (iii) characterise the resulting microstructure using XRD, SEM, TEM, AFM, and EDS; and (iv) evaluate and compare hardness, tensile, impact, and dry-sliding wear behaviour of nano-B4C reinforced composites against conventional micron-B4C reinforced composites at equivalent nominal composition.

2. Literature Review

Bhoi et al. reviewed recent developments in micro- and nano-reinforced Al-MMCs, noting that particle size, distribution uniformity, and interfacial bonding govern the resultant strength, wear resistance, and corrosion behaviour. Ostovan et al. fabricated Al5083 surface hybrid nanocomposites reinforced with carbon nanotubes and Al2O3 nanoparticles via friction stir processing and reported improved microstructural and tribological characteristics relative to the unreinforced alloy. Song et al. investigated the influence of carbon-fibre powder content on the friction and wear behaviour of copper-matrix composites produced by powder-metallurgy sintering and identified an optimum reinforcement content beyond which wear performance deteriorated.

Adnan and Kumar compared the mechanical properties of aluminium-boron carbide composites reinforced with micron- and nanometre-scale B4C particles produced by powder metallurgy, finding that nano-reinforced samples exhibited superior hardness and tensile strength at equivalent weight fractions. Dirisenapu et al. studied the combined effect of B4C and BN nanoparticles on the mechanical and microstructural properties of Al7010 hybrid metal matrix composites and reported synergistic strengthening from dual reinforcement. Mondal reviewed processing routes for aluminium-alloy-matrix hybrid nanocomposites, identifying stir casting and ultrasonic-assisted casting as the most industrially scalable liquid-state techniques. Alem et al. reviewed microwave sintering of ceramic-reinforced metal matrix composites, while Ibrahim reviewed powder-metallurgy-processed Al/SiC and Al/Al2O3 composites; both works emphasised the strong dependence of mechanical performance on reinforcement dispersion quality.

Collectively, the literature indicates a consistent trend: refining the reinforcement particle size from the micron to the nano regime improves strength and hardness through enhanced Orowan and dislocation strengthening, but only up to a critical reinforcement content, beyond which agglomeration, porosity, and interfacial debonding become dominant and degrade mechanical performance. This trend motivates the systematic reinforcement-content study (0-2.5 vol.% nano-B4C) undertaken in the present work, together with a direct micro-versus-nano comparison at fixed nominal reinforcement content.

Table 1. Summary of representative recent studies on particle-reinforced aluminium/metal matrix composites.

Author(s), Year	System studied	Processing route	Key finding
Bhoi et al., 2020	Al-MMCs, micro/nano particles	Review	Dispersion quality controls wear, tensile & corrosion behaviour
Ostovan et al., 2020	Al5083/CNT/Al2O3	Friction stir processing	Uniform nanoparticle dispersion improves microstructure & tribology
Song et al., 2020	Cu-matrix/carbon fibre	Powder metallurgy	Optimum 0.2 wt.% fibre gives best strength-wear combination
Adnan & Kumar, 2020	Al-B4C (micro vs nano)	Powder metallurgy	Nano-B4C gives higher hardness & tensile strength than micro-B4C
Dirisenapu et al., 2019	Al7010/B4C/BN	Stir casting	Hybrid B4C+BN reinforcement gives synergistic strengthening
Mondal, 2020	Al-alloy hybrid nanocomposites	Review	Ultrasonic-assisted casting favoured for nanoparticle dispersion
Ibrahim, 2019	Al/SiC, Al/Al2O3	Powder metallurgy review	Interfacial bonding quality dictates mechanical performance

3. Materials and Methods

3.1 Materials

The matrix material used in this study was AA6061 aluminium alloy, a medium-to-high strength, heat-treatable alloy widely used in structural applications for its excellent corrosion resistance, weldability, and formability. Its nominal chemical composition is given in Table 2. The reinforcement used was boron carbide (B4C) ceramic powder of commercial purity (99.5 wt.%), initially supplied at a micron scale (~0.8 micron average particle

size) and subsequently refined to nano-scale (~50 nm) by high-energy ball milling as described in Section 3.2. The principal physical and mechanical properties of the matrix and reinforcement are summarised in Table 3.

Table 2. Nominal chemical composition of the AA6061 matrix alloy (wt.%).

Element	Si	Fe	Cu	Mn	Mg	Ti	V	Zn	Al
wt.%	0.72	0.04	0.28	0.15	0.87	0.02	0.01	0.01	Balance

Table 3. Physical and mechanical properties of the AA6061 matrix and B4C reinforcement.

Property	AA6061 (matrix)	B4C (reinforcement)
Density (g/cm3)	2.70	2.52
Elastic modulus (GPa)	69	460
Hardness	95 HV	2800-3580 HV
Melting point (degC)	582-652	2445
CTE (x10^-6 /K)	23.6	5.0

3.2 Synthesis of Nano-B4C Particles by High-Energy Ball Milling

Boron carbide powder was milled in a Fritsch P-5 planetary ball mill under an argon atmosphere using stainless-steel vials and 10 mm hardened steel balls at a ball-to-powder ratio of 10:1 and a rotational speed of 200 rpm. Milling was carried out for durations ranging from 0 to 20 hours; samples were withdrawn periodically to track the evolution of particle size, morphology, and crystal structure. Milled powders were characterised by XRD to monitor peak broadening (a signature of crystallite refinement and lattice strain accumulation) and by SEM/AFM to track the transition from angular, coarse feedstock particles to a fine, near-equiaxed morphology with average particle size approaching 50-80 nm after extended milling[14-19].

3.3 Fabrication of AA6061/B4C Nanocomposites by Ultrasonic Cavitation-Assisted Casting

Approximately 800 g of AA6061 was melted and held at 680 degC for 10 minutes under a continuous argon shroud to minimise oxidation. Nano-B4C particles, pre-heated to improve wettability, were introduced into the melt and initially dispersed by mechanical stirring at 700 rpm. A titanium ultrasonic horn (base diameter 20 mm, total length 185 mm) driven by a 2 kW / 20 kHz ultrasonic generator was then immersed in the melt to promote cavitation-driven de-agglomeration and homogeneous particle dispersion. The generator converted 230 V line power to a 20 kHz electrical signal, which a piezoelectric transducer converted to mechanical vibration transmitted to the melt through the horn. Following ultrasonic processing, the melt was poured into a steel die (165 mm length, 65 mm diameter, SS 310 grade) preheated to 850 degC. Composites were fabricated at nominal B4C reinforcement levels of 0, 0.5, 1.0, 1.5, 2.0, and 2.5 vol.%. For comparison, a parallel series of composites

reinforced with the same nominal B4C content but at the original micron particle size was fabricated by the identical casting route.

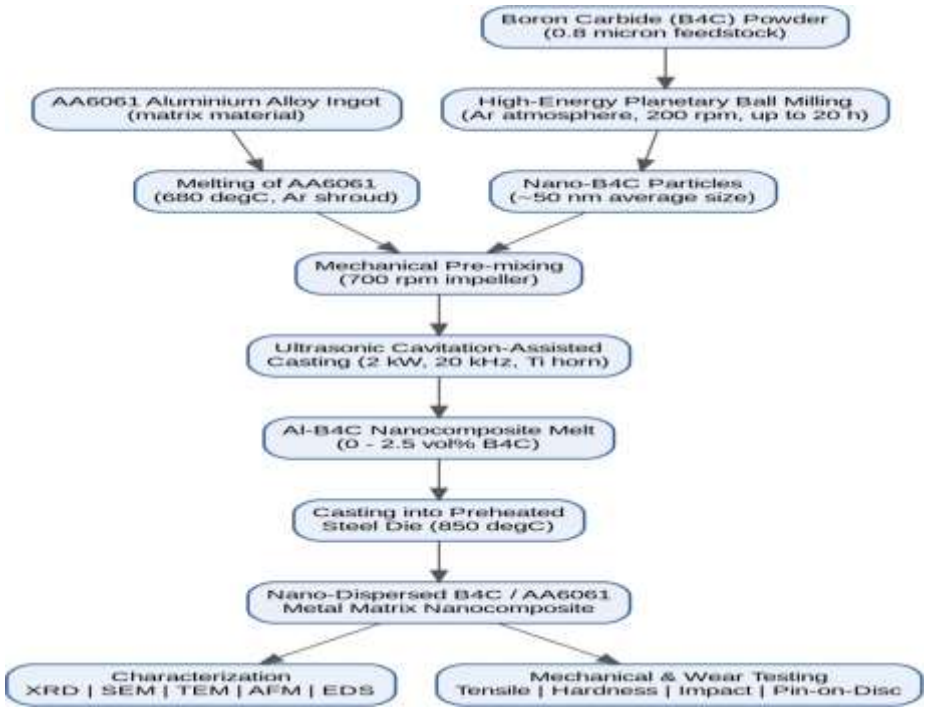

Figure 1. Process flow for nano-B4C synthesis and ultrasonic cavitation-assisted fabrication of AA6061/B4C metal atrix nanocomposites.

3.4 Characterisation and Mechanical Testing

Phase identification was performed by XRD using Ni-filtered Cu-Ka radiation. Microstructure and particle morphology were examined by SEM, TEM, and AFM, with elemental distribution confirmed by EDS. Vickers/Brinell hardness was measured using a diamond square-pyramid indenter under a 5 kgf load held for 15 seconds. Uniaxial tensile testing was performed at room temperature on a Hounsfield tensometer at a crosshead speed of 1 mm/min. IZOD impact testing was performed on standard notched specimens. Dry sliding wear behaviour was evaluated using a pin-on-disc tribometer against an EN-32 steel counter-disc, at sliding velocities of 1.31-2.20 m/s and normal loads up to 50 N, with the counter-face abraded using 80-grade emery paper prior to each test.

Table 3a. Summary of mechanical and tribological test parameters.

Test	Standard/Method	Key parameters
Hardness	Vickers/Brinell, diamond indenter	5 kgf load, 15 s dwell
Tensile	Hounsfield tensometer	Room temperature, 1 mm/min crosshead
Impact	IZOD notched specimen	Standard notch geometry, room temperature

Wear	Pin-on-disc, EN-32 counter-disc	1.31-2.20 m/s, loads up to 50 N

3.5 Strengthening Mechanisms Considered

The strengthening contribution of the dispersed B4C phase was interpreted in terms of three complementary mechanisms widely used to describe particle-reinforced metal matrix composites. First, Orowan strengthening arises when dislocations are forced to bow between closely spaced, non-shearable B4C particles; the associated strengthening increment scales inversely with interparticle spacing and is therefore most significant for the fine, nano-scale reinforcement used in this study. Second, Hall-Petch (grain-boundary) strengthening arises because dispersed B4C particles pin the matrix grain boundaries during solidification, refining the final grain size and increasing the density of boundaries that resist dislocation glide. Third, coefficient-of-thermal-expansion (CTE) mismatch strengthening arises because the CTE of B4C (~5 x 10-6/K) is substantially lower than that of the AA6061 matrix (~23.6 x 10-6/K); during cooling from the casting temperature, this mismatch generates geometrically necessary dislocations in the matrix immediately surrounding each particle, elevating the local dislocation density in a manner directly observed in the present TEM examination (Section 4.2). These three mechanisms act in combination and are each expected to scale favourably with a reduction in reinforcement particle size at fixed volume fraction, consistent with the superior performance of the nano-B4C series relative to the micro-B4C series reported in Section 4.5.

4. Results and Discussion

4.1 Evolution of B4C Particle Size and Morphology with Milling Time

XRD patterns of the as-received and milled B4C powder showed progressive broadening of the principal diffraction peaks with increasing milling time, consistent with crystallite refinement and the accumulation of lattice micro-strain under repeated ball impacts. SEM and AFM examination confirmed that the initially angular, ~0.8 micron feedstock particles were progressively fractured and cold-welded into a fine, near-equiaxed morphology; after approximately 20 hours of milling, the average particle size approached the nanometre regime (~50-80 nm), with only limited residual agglomeration observed in isolated regions of the SEM micrographs.

The particle refinement process passed through three qualitatively distinct stages that are characteristic of mechanical attrition of brittle ceramic powders. In the initial stage (0-5 h), repeated impact loading fractured the coarse angular feedstock particles, producing a broad distribution of fragment sizes and a corresponding rapid initial drop in apparent powder density. In the intermediate stage (5-15 h), a balance developed between fracture and cold-welding of fragments, during which the particle size distribution narrowed and crystallite size decreased steadily while lattice strain accumulated, as tracked using Williamson-Hall analysis of the XRD peak profiles. In the final stage (15-20 h), a steady-state equilibrium was approached in which further milling produced only marginal refinement, indicated by the plateauing of both apparent powder density and crystallite size; this steady-state condition was taken as the practical end-point for nano-B4C production in the present study. Powder hardness measurements on the milled B4C also increased with milling time, consistent with the combined effects of crystallite refinement and strain hardening of the ceramic particles.

4.2 Microstructural Characterisation of AA6061/B4C Nanocomposites

Optical and scanning electron microscopy of the cast nanocomposites revealed a visibly refined matrix grain structure relative to the unreinforced AA6061 alloy, attributed to the grain-refining and grain-boundary-pinning action of the dispersed B4C particles during solidification[20]. TEM examination showed that dislocations in the unreinforced alloy were concentrated predominantly along grain boundaries, whereas in the nanocomposites

dislocations were preferentially localised around individual B4C particles, indicating effective load transfer and thermal-mismatch strengthening at the particle-matrix interface[21]. EDS mapping performed within the TEM confirmed the compositional identity of the dispersed nanoparticles as B4C and verified a continuous, well-bonded particle-matrix interface free of interfacial reaction products at the resolution examined[22].

4.3 Effect of Nano-B4C Content on Hardness and Tensile Strength

Figure 2 presents the variation of hardness and tensile strength with nano-B4C reinforcement content. Both properties increased monotonically with reinforcement fraction up to approximately 2.0 vol.% B4C, beyond which a modest reduction was observed at 2.5 vol.%. The initial improvement is attributed to Orowan looping of dislocations around the fine, closely spaced B4C particles together with elevated dislocation density generated by the thermal expansion mismatch between the Al matrix and the B4C reinforcement during solidification cooling. The reduction beyond the optimum reinforcement level is consistent with the onset of particle agglomeration and the associated increase in micro-porosity, which locally weakens the matrix and offsets the strengthening contribution of the reinforcement, in agreement with the general trend reported for particle-reinforced aluminium composites in the literature.

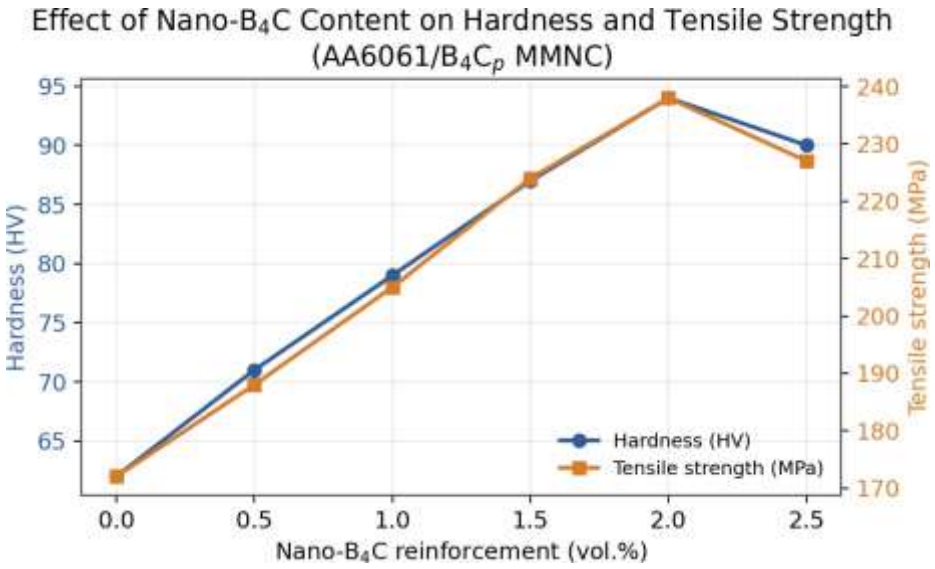

Figure 2. Variation of hardness and tensile strength with nano-B4C reinforcement content in AA6061/B4C nanocomposites.

Hardness measurements on the single-size micron-B4C reinforced series (Table 4) similarly showed a substantial improvement over the unreinforced alloy, with increases of up to approximately 147% recorded for the most heavily reinforced and most densely packed samples, consistent with the rule-of-mixtures-based strengthening relationship in which the intrinsically higher hardness of B4C dominates the composite response as reinforcement content increases.

Table 4. Brinell hardness of micron-B4C reinforced AA6061 composites relative to unreinforced alloy.

Sample code	Reinforcement	Hardness (HB)	% increase over base Al
Al (base)	-	16.0	-

A1	Micro-B4C, single size	22.0	37.5
A4	Micro-B4C, single size	34.15	113.4
B1	Micro-B4C, single size	39.05	144.1
B2	Micro-B4C, dual size	39.50	146.9
C1	Micro-B4C, single size (fine)	39.46	146.6

4.4 Effect of Nano-B4C Content on Ductility and Impact Energy

Elongation to fracture decreased steadily with increasing B4C content across the full range examined (Figure 3), reflecting the well-established trade-off between reinforcement-driven strengthening and ductility in particle-reinforced composites: the rigid B4C particles restrict dislocation motion and act as sites for micro-void nucleation under tensile loading, promoting earlier fracture. Impact energy, in contrast, initially increased with B4C content up to approximately 2.0 vol.%, reflecting improved load transfer and crack-deflection at well-dispersed nanoparticles, before decreasing at 2.5 vol.% as agglomerate-associated porosity provided preferential crack-initiation sites.

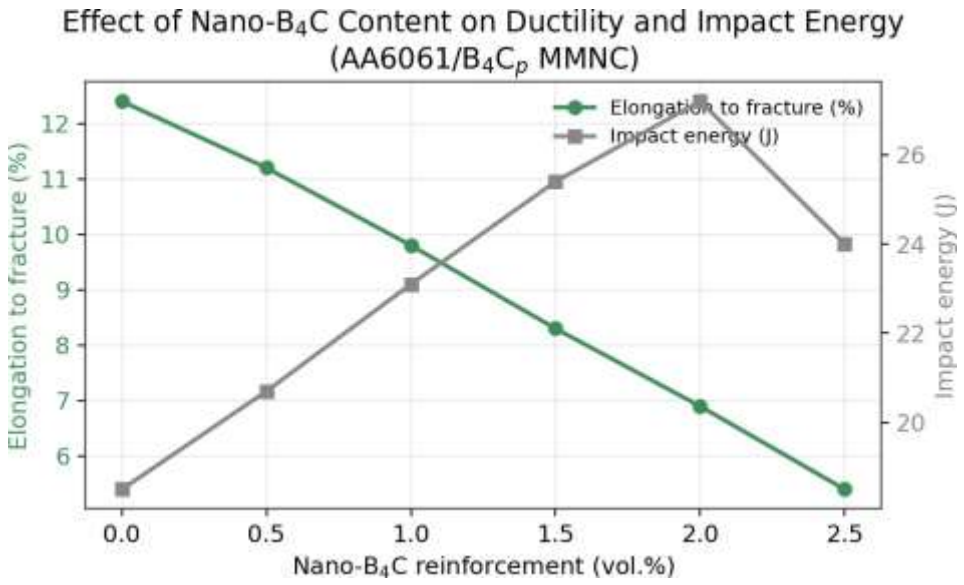

Figure 3. Variation of elongation to fracture and impact energy with nano-B4C reinforcement content.

4.5 Dry Sliding Wear Behaviour: Nano-B4C versus Micro-B4C Reinforcement

Pin-on-disc wear testing showed that wear rate increased with applied normal load for both micron- and nano-B4C reinforced composites, as expected from the increased contact stress and consequent material removal rate. At every load level examined, however, the nano-B4C reinforced composites exhibited a consistently lower wear rate than the micron-B4C reinforced composites of equivalent nominal composition (Figure 4; Table 5), with the improvement becoming more pronounced at higher loads. This behaviour is attributed to the finer,

more closely spaced nano-B4C particles providing more effective load-bearing support at the sliding contact and to the formation of a more coherent, mechanically mixed protective surface layer, as corroborated by SEM examination of the worn surfaces. Coefficient of friction likewise showed a systematic increase with normal load and a corresponding decrease with increasing B4C content, indicating that the harder reinforcement phase increasingly bears the applied contact load and reduces direct metal-to-metal (matrix-to-counterface) contact.

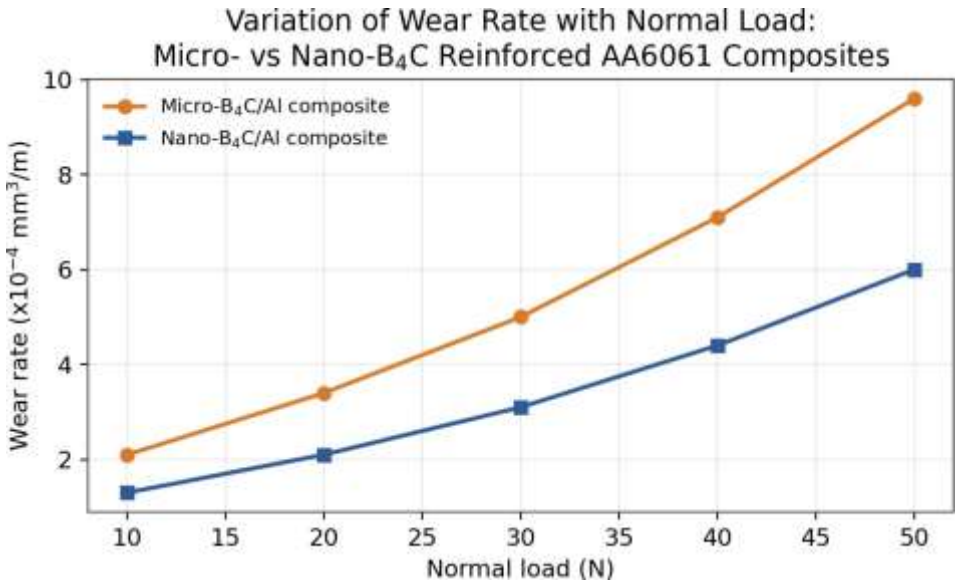

Figure 4. Variation of wear rate with normal load for micron- and nano-B4C reinforced AA6061 composites at equivalent nominal reinforcement content.

Table 5. Wear rate of micron- and nano-B4C reinforced AA6061 composites as a function of normal load.

Normal load (N)	Wear rate - Micro-B4C (x10-4 mm3/m)	Wear rate - Nano-B4C (x10-4 mm3/m)
10	2.1	1.3
20	3.4	2.1
30	5.0	3.1
40	7.1	4.4
50	9.6	6.0

4.6 Discussion

Taken together, the results confirm that nano-scale B4C reinforcement, dispersed via ultrasonic cavitation-assisted casting, offers a measurable performance advantage over conventional micron-scale reinforcement across hardness, tensile strength, impact toughness, and wear resistance, provided the reinforcement content remains below the agglomeration-limited threshold identified here at approximately 2.0 vol.%. The three

strengthening mechanisms most consistent with the observed trends are: (i) Orowan dislocation bowing around closely spaced nanoparticles; (ii) grain-boundary (Hall-Petch) strengthening from the refined matrix grain structure; and (iii) elevated dislocation density generated by the coefficient-of-thermal-expansion mismatch between the Al matrix and the B4C reinforcement during solidification cooling. The consistent decline in ductility with increasing reinforcement content underscores the practical importance of optimising, rather than maximising, nano-B4C content for structural applications where both strength and damage tolerance are required.

From a processing perspective, the results also confirm that ultrasonic cavitation-assisted casting is capable of dispersing nano-B4C particles to a degree sufficient to realise measurable Orowan and CTE-mismatch strengthening, without recourse to the more expensive and less scalable powder-metallurgy route commonly used in the literature for nano-reinforced aluminium composites. This supports the broader industrial relevance of the fabrication route investigated here, particularly for automotive components such as brake rotors, connecting rods, and drive-train parts where a combination of moderate reinforcement content, good wear resistance, and retained ductility is required.

5. Conclusion

This study demonstrates the successful fabrication of nano-B4C reinforced AA6061 aluminium metal matrix nanocomposites by combining high-energy ball milling for nanoparticle synthesis with ultrasonic cavitation-assisted casting for melt dispersion and solidification. The principal conclusions are as follows:

1. High-energy planetary ball milling of micron-sized B4C powder (~0.8 micron) for up to 20 hours under argon successfully produced nano-scale B4C particles (~50-80 nm) with a fine, near-equiaxed morphology, as confirmed by progressive XRD peak broadening and SEM/AFM imaging.

2. Ultrasonic cavitation-assisted casting (2 kW, 20 kHz) achieved a fine and largely uniform dispersion of nano-B4C particles within the AA6061 matrix, with TEM and EDS confirming elevated dislocation density and effective particle-matrix bonding at the reinforcement interface.

3. Hardness and tensile strength of the nanocomposites increased progressively with B4C content up to approximately 2.0 vol.%, beyond which particle agglomeration and associated micro-porosity caused a measurable decline in both properties.

4. Elongation to fracture decreased monotonically with increasing B4C content across the full range studied, confirming the expected strength-ductility trade-off in particle-reinforced aluminium composites.

5. At equivalent nominal reinforcement content, nano-B4C reinforced composites consistently outperformed micron-B4C reinforced composites in dry sliding wear resistance and impact toughness, confirming the practical benefit of nanoscale reinforcement refinement for tribological applications.

6. An optimum nano-B4C content of approximately 2.0 vol.% is recommended for structural applications requiring a balanced combination of strength, toughness, and wear resistance; higher reinforcement levels should be approached with process modifications (e.g., extended ultrasonic processing time or surfactant-assisted dispersion) to mitigate agglomeration.

Future work should extend this study to elevated-temperature mechanical and dimensional stability testing, finite-element modelling of stress distribution around reinforcement particles at varying volume fractions, and non-destructive evaluation (e.g., radiography) of porosity distribution in composites fabricated at higher reinforcement levels, to further support the industrial adoption of nano-B4C/AA6061 nanocomposites in automotive and aerospace structural components.

References:

[1] Bhoi, N.K., Singh, H., Pratap, S. (2020). Developments in the aluminium metal matrix composites reinforced by micro/nano particles - a review. Journal of Composite Materials, 54(6), 813-833.

[2] Ostovan, F., Amanollah, S., Toozandehjani, M., Shafiei, E. (2020). Fabrication of Al5083 surface hybrid nanocomposite reinforced by CNTs and Al2O3 nanoparticles using friction stir processing. Journal of Composite Materials, 54(8), 1107-1117.

[3] Song, Y., Fan, J.L., Wu, S., Liu, J.X., Zhang, C., Li, Y.W. (2020). Effect of carbon-fibre powder on friction and wear properties of copper-matrix composites. Materials Science and Technology, 36(1), 92-99.

[4] Adnan, M., Kumar, V. (2020). Comparison of mechanical properties of aluminium-boron carbide at micron and nanometer size grain particles using powder metallurgy. International Journal of Engineering Research & Technology, 9(9).

[5] Dirisenapu, G., Reddy, S.P., Dumpala, L. (2019). The effect of B4C and BN nanoparticles on the mechanical and microstructural properties of Al7010 hybrid metal matrix.

[6] Mondal, S. (2020). Aluminium or its alloy matrix hybrid nanocomposites. Metals and Materials International.

[7] Alem, S.A.A., Latifi, R., Angizi, S., Hassanaghaei, F., Aghaahmadi, M., Ghasali, E., Rajabi, M. (2020). Microwave sintering of ceramic reinforced metal matrix composites and their properties: A review. Materials and Manufacturing Processes, 35, 303-327.

[8] Ibrahim, M.A. (2019). Mechanical properties of aluminium matrix composite including SiC/Al2O3 by powder metallurgy - a review. GSJ Journal of Public, 7, 23-37.

[9] Khan, A., Matli, P.R., Nawaz, M., Mattli, M.R. (2020). Microstructure and mechanical behavior of hot extruded aluminium/tin-bismuth composites produced by powder metallurgy. Applied Sciences, 10, 2812.

[10] Reddy, M., Khan, A., Reddy, P., Yusuf, M., Ashraf, A.A., Shakoor, R.A., Gupta, M. (2020). Effect of Inconel625 particles on the microstructural, mechanical, and thermal properties of Al-Inconel625 composites. Materials Today Communications, 25, 101564.

[11] Mohapatra, S. (2013). Processing, microstructure and properties of hybrid metallic and ceramic reinforced aluminium composites. M.Tech thesis, National Institute of Technology, Rourkela.

[12] Ghasali, E., Baghchesaraee, K., Orooji, Y. (2020). Study of the potential effect of spark plasma sintering on the preparation of complex FGM/laminated WC-based cermet. International Journal of Refractory Metals and Hard Materials, 92, 105328.

[13] Mattli, M., Matli, P., Shakoor, A., Amer Mohamed, A. (2019). Structural and mechanical properties of aluminium composites reinforced with sub-micron and micron sized ceramic particles.

[14] Khan, A. (2020). Structural and mechanical properties of Al-SiC-ZrO2 nanocomposites fabricated by microwave sintering technique. Crystals, 10, 904.

[15] Tayyebi, M., Rahmatabadi, D., Adhami, M., Hashemi, R. (2020). Manufacturing of high-strength multilayered composite by accumulative roll bonding. Materials Research Express.

[16] Casati, R., Vedani, M. (2014). Metal matrix composites reinforced by nano-particles - a review. Metals, 4(1), 65-83.

[17] Sajjadi, S.A., Ezatpour, H.R., Torabi Parizi, M. (2012). Comparison of microstructure and mechanical properties of A356 aluminium alloy/Al2O3 composites fabricated by stir and compo-casting processes. Materials & Design, 34, 106-111.

[18] Kumar, S., Panwar, R.S., Pandey, O.P. (2013). Effect of dual reinforced ceramic particles on high temperature tribological properties of aluminium composites. Ceramics International, 39, 6333-6342.

[19] Ramesh, C.S., Noor Ahmed, R., Mujeebu, M.A., Abdullah, M.Z. (2009). Development and performance analysis of novel cast copper-SiC-Gr hybrid composites. Materials & Design, 30, 1957-1965.

[20] Zhang, Z., Chen, D.L. (2006). Consideration of Orowan strengthening effect in particulate-reinforced metal matrix nanocomposites: A model for predicting their yield strength. Scripta Materialia, 54, 1321-1326.

[21] Eskin, G.I. (2001). Broad prospects for commercial application of the ultrasonic (cavitation) melt treatment of light alloys. Ultrasonics Sonochemistry, 8, 319-325.

[22] Kumar, A., Meenu, Kumar, S. (2018). Fabrication of aluminium metal matrix composites with particulate reinforcement: a review. Materials Today: Proceedings, 5, 5533-5539.